

## INFLUENCE OF THERMAL TREATMENT ON STRUCTURAL PROPERTIES OF SOME ZINC-PHOSPHATE GLASSES DOPED WITH IRON IONS

LIVIU CALIN BOLUNDUT<sup>a\*</sup> AND VASILE POP<sup>a</sup>

**ABSTRACT.** Glass ceramics samples with chemical composition  $(\text{Fe}_2\text{O}_3)_x \cdot (\text{P}_2\text{O}_5)_{40} \cdot (\text{ZnO})_{(60-x)}$  ( $0 \leq x \leq 20$  mol%) were prepared by melt-quenching technique, followed by a thermal treatment at two different temperatures for two hours. Structural properties were studied by DTA, XRD, and FTIR measurements. From DTA measurements can be observed that, with increasing in concentration of the dopant ( $\text{Fe}_2\text{O}_3$ ), the transition and crystallization temperatures increase. The XRD data show, the presence of two or three crystalline phases, and the FTIR data confirm the existence of  $\text{ZnO}_4$  structural units in our samples. So the thermal treatment applied to the samples lead to changes in the structural properties and also to some modification in the glass ceramic network.

**Keywords:** zinc phosphate glass ceramics, DTA, XRD, transitional metals doped glass ceramics.

### INTRODUCTION

Due to their multiple applications and important physical properties, phosphate glasses have fascinated the researchers in the recent years. This kind of materials have potentials applications in a great diversity of technology areas such as: optical and magnetic devices [1], bio-materials [2, 3], memory switching [4], electronics [5, 6], matrix for containment of the waste [7], energy transfer materials [8], battery materials [9], solid state laser hosts [10, 11], etc. Also, the phosphate glasses have some limits due to their poor chemical durability. The presence of water will destroy the P-O-P bonds from the glass network, so the use of this kind of glasses under hydrated conditions is limited [12, 13]. The adding of transition metal ions, in the phosphate glass matrix, will lead to the

---

<sup>a</sup> Technical University of Cluj-Napoca, Faculty of Materials and Environmental Engineering, Physics and Chemistry Department 28 Memorandumului str., RO-400114, Cluj-Napoca, Romania

\* Corresponding author: liviu.bolundut@chem.utcluj.ro

improving of the chemical durability. When metal ions are incorporated in the glass network, are produced some structural changes. These ions will replace some phosphorus atoms and will form P-O-M<sup>n+</sup> bonds that are more stable at the water presence [14-16]. This behavior increase the sphere of applications for phosphate glasses.

As example of glasses with transition metals ions, can be mentioned the zinc phosphate and zinc boro-phosphate glasses [14, 15].

In the zinc phosphate glasses, zinc ions act as network modifier, in this way this kind of glasses have a high transparency in the UV region and can be used at the fabrication of liquid crystal screens and withe light-emitting diodes [11].

Glasses containing transition metal ions are also important from scientific point of view due to the presence of free electrons in d orbitals or the presence of free d orbitals at the metallic ions. This cause the modifications of the coordination number, bonding characteristics, covalence state of the substituents metal ions and of the glass networks. All this studies are very helpful in understanding the structure of glassy state [17].

The aim of this work was to obtain some zinc phosphate glasses doped with iron (III) oxide (Fe<sub>2</sub>O<sub>3</sub>) and investigate them by DTA, XRD, and FTIR measurements in order to establish the structural changes produced by the heat treatments at different temperatures applied to all obtained samples.

## RESULTS AND DISCUSSION

DTA (Differential Thermal Analysis) measurements are important because in this way can be determined the glass characteristic temperatures such as: melting temperature  $T_m$ , glass transition temperature  $T_g$  and crystallization temperature  $T_c$ . Using these parameters can be estimated for example the thermal stability of the glasses according with the literature [17-20].

The figure 1 present the DTA curves, for our obtained samples, at the heating rate of 15 °C/minute.

The DTA curve for the glass matrix ( $x = 0$  mol%) show a weak glass transition around temperature of 412 °C, a peak situated at 667 °C, for a slow crystallization process, followed by another two endothermic effects corresponding to the melting of material in two steps that are situated at 776 and 796 °C.

In the case of samples that contain a high concentration of iron ions ( $x = 10$  mol%) a clear glass transition can be observed and also the increase of the transition temperature at 451 °C. On the other hand seems to appear two exothermic effects corresponding to crystallization processes (due to the formation of two crystalline phases) around of 681 and 758 °C, followed by two endothermic ones at 872 and 911 °C due to the melting of material.

For the sample with 20 mol% of iron (III) oxide can be observed that the glass transition and the crystallization temperatures increase.

Also the figure 1 present a single peak due to the glass transition temperature ( $T_g$ ), indicating the homogeneity of the all obtained samples.

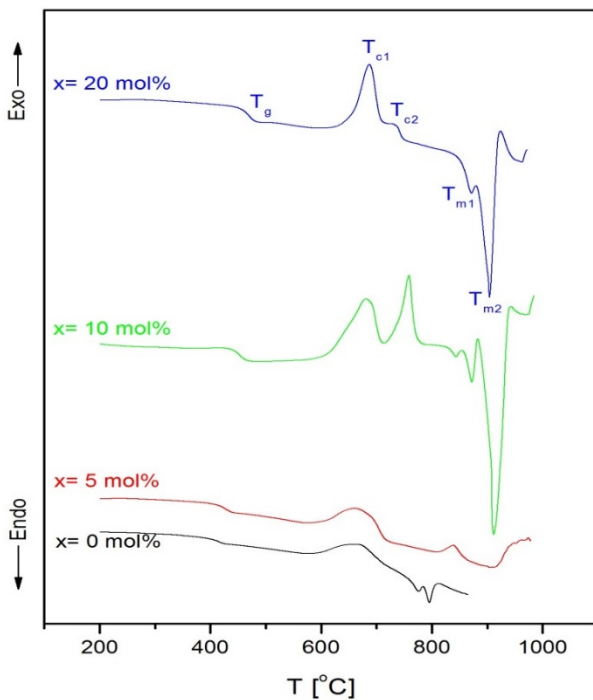


**Figure 1.** The DTA curves of the  $(Fe_2O_3)_x \cdot (P_2O_5)_{40} \cdot (ZnO)_{(60-x)}$  glasses

For our samples were been calculated some parameters such as: activation energy of vitreous transition ( $E_g$ ), activation energy at crystallization ( $E_c$ ), fragility index ( $F$ ), thermal stability ( $TS$ ) and glass stability ( $S$ ), parameters that arte listed in table 1.

**Table 1.** The glass characteristic temperatures ( $T_g$ ,  $T_c$ ,  $T_m$ ), stability parameters ( $TS$ ,  $S$ ) and activation energies ( $E_g$ ,  $E_c$ ) for the studied  $(Fe_2O_3)_x \cdot (P_2O_5)_{40} \cdot (ZnO)_{(60-x)}$  ( $0 \leq x \leq 20$  mol%) glasses

x	$T_g$ [°C]	$T_{c1}$ [°C]	$T_{c2}$ [°C]	$T_{m1}$ [°C]	$T_{m2}$ [°C]	TS [°C]	S [°C]	F	$E_g$ [kJ/mol]	$E_c$ [kJ/mol]
0	412	667	-	776	796	195	35,7	20,2	264,4	176,3
5	427	672	-	807	909	183	26,6	37,8	309,2	267,1
10	451	681	758	872	911	168	23,1	47,3	408,3	310,4
20	469	687	734	871	904	163	19,1	50,1	449,7	335,4

The thermal stability (TS) was introduced by Dietzel [18] and is expressed by the equation:

$$TS = T_c - T_g \quad (1)$$

Glass stability parameter (S) introduced by Saad and Poulin [20] was calculated using the relation:

$$S = \frac{(T_p - T_c) \cdot (T_c - T_g)}{T_g} \quad (2)$$

Another parameter was the fragility index that can be obtained using the equation [21]:

$$F = \frac{E_g}{R \cdot T_g \cdot \ln 10} \quad (3)$$

Activation energy of the studied glasses was calculated using the Kissinger formula [22]:

$$\ln\left(\frac{T_g^2}{\beta}\right) = \frac{E_g}{R \cdot T_g} + const. \quad (4)$$

where  $\beta$  represent the heating rate of DTA ( $\beta = 5, 10, 15, 20, 25$  °C/minute), and R is the gas constant.

These parameters express the stability and fragility of the obtained samples, and also provide information about structural changes that take place in the glass ceramic network.

From table 1 can be observed that the glass matrix has the highest thermal stability indicated by all glass stability parameters. Increasing the doping level with iron ions by adding of the  $Fe_2O_3$  leads to the decrease of glass stability probably due to some changes that take place in the glass ceramic network (increase the number of non-bridging oxygen). Also, when iron(III) oxide is introduced, the P-O-P bonds are transformed in Fe-O-P bonds and the chemical character of the bonds from the glass network is modified. The ionic character of the bonds increase and the glasses became more fragile according with the literature data [21].

In figure 2a and 2b are presented the dependences  $\ln(T_g^2/\beta)$  versus  $10^3/T_g$  and  $\ln(T_c^2/\beta)$  versus  $10^3/T_c$  for the investigated samples.

From the slopes of the  $\ln(T_g^2/\beta)$  versus  $10^3/T_g$  and  $\ln(T_c^2/\beta)$  versus  $10^3/T_g$  graphics can be determined  $E_g$  and  $E_c$  activation energies for the studied samples. In our case the activation energy of vitreous transition ( $E_g$ ) and the activation energy at crystallization ( $E_c$ ) increase with the increasing of the doping level (the concentration of  $Fe_2O_3$ ).

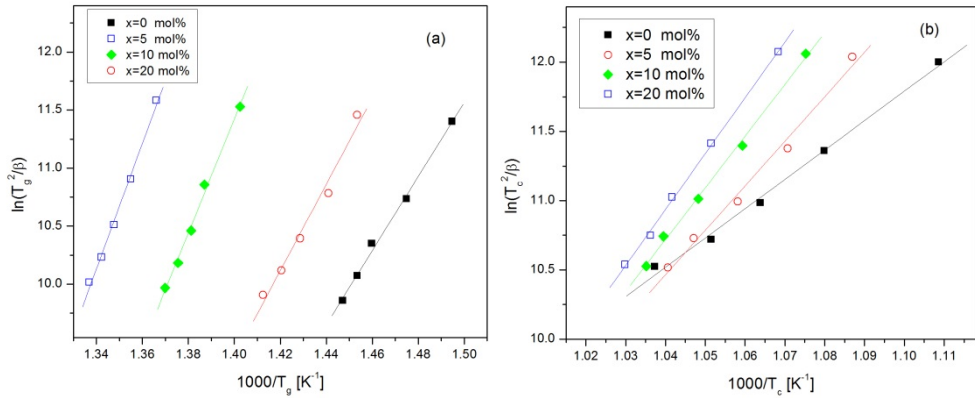


**Figure 2a and 2b.** The dependences  $\ln(T_g^2/\beta)$  on  $10^3/T_g$  for the  $(\text{Fe}_2\text{O}_3)_x \cdot (\text{P}_2\text{O}_5)_{40} \cdot (\text{ZnO})_{(60-x)}$  glasses and the dependences  $\ln(T_c^2/\beta)$  on  $10^3/T_c$  for the  $(\text{Fe}_2\text{O}_3)_x \cdot (\text{P}_2\text{O}_5)_{40} \cdot (\text{ZnO})_{(60-x)}$  glasses

The activation energy of glass transition ( $E_g$ ) seems to be responsible for the molecular motion and rearrangements of the atoms around  $T_g$  temperature. According with the literature, a small value of  $E_g$  lead to a stable glass sample [23]. So in our case, the sample with the smallest  $E_g$  (the most stable one, from this point of view) is the matrix.

The XRD patterns obtained for the studied samples of the glass system  $(\text{Fe}_2\text{O}_3)_x \cdot (\text{P}_2\text{O}_5)_{40} \cdot (\text{ZnO})_{(60-x)}$  annealed for two hours at different temperatures are shown in figure 3.

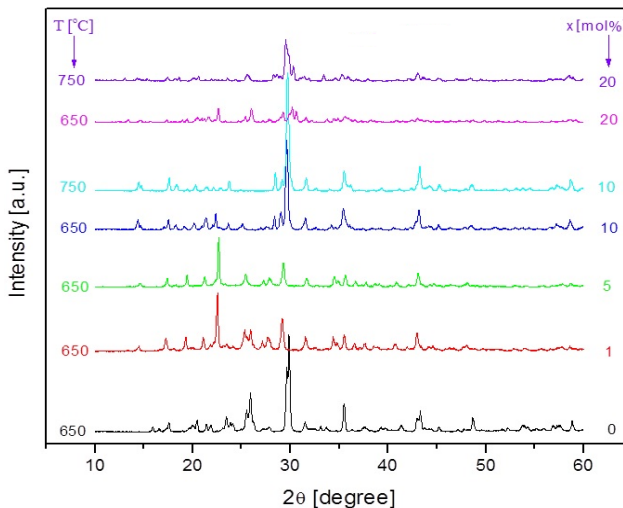


**Figure 3.** The XRD patterns of  $(\text{Fe}_2\text{O}_3)_x \cdot (\text{P}_2\text{O}_5)_{40} \cdot (\text{ZnO})_{(60-x)}$  glass ceramics

The matrix  $(P_2O_5)_{40} \cdot (ZnO)_{60}$  annealed for two hours at  $650\text{ }^\circ\text{C}$  contain two crystalline phases  $Zn_2P_2O_7$  (PDF:34-1275) and  $Zn(PO_3)_2$  (PDF:30-1488) and the degree of crystallinity for this sample is 71.78%. The degree of crystallinity degree was calculated using Reflex computer program part of Material Studio software [24]. For the samples with concentration of iron (III) oxide equal or higher than  $x = 10\text{ mol}\%$  was identified another crystalline phase that contain iron ( $ZnFe_2O_4$  PDF:74-2397). In the table 2 is listed the evolution of crystalline phases obtained for the studied samples that were annealed for two hours at different temperatures.

**Table 2.** The crystalline phases evolution for the studied samples

x [mol%]	T <sub>tt</sub> [°C]	Crystalline Phase
0	650	$Zn_2P_2O_7$ , $Zn(PO_3)_2$
3	650	$Zn_2P_2O_7$ , $Zn(PO_3)_2$
5	650	$Zn_2P_2O_7$
10	650	$Zn_2P_2O_7$ , $ZnFe_2O_4$
10	750	$Zn_2P_2O_7$ , $ZnFe_2O_4$
20	650	$Zn_2P_2O_7$ , $ZnFe_2O_4$ , $Zn(PO_3)_2$
20	750	$Zn_2P_2O_7$ , $ZnFe_2O_4$ , $Zn(PO_3)_2$

The thermally untreated samples, present XRD patterns that show an amorphous nature of the samples up to a concentration of iron(III) oxide  $x < 30\text{ mol}\%$ . For the sample with iron (III) oxide content of  $30\text{ mol}\%$  was observed a large halo and peaks characteristic to  $FePO_4$  crystalline phase [25]. Due to all mentioned above, the heat treatment increase the degree of crystallinity and also make important changes in the glass ceramic network of the samples.

These changes can be proved also by FTIR measurements that are presented in figure 4a.

The IR spectra were deconvoluted (using a Gaussian type function) in order to obtain some information about the type of structural groups that are present in our glass ceramic network. Also the deconvoluted spectra help us to see the influence of the heat treatment on these structural units (by assignments of the IR vibrations) and the changes that take place in the glass ceramic network. For example we present the deconvolution in case of glass ceramic matrix and for the sample doped with  $5\text{ mol}\%$  of  $Fe_2O_3$  (figure 5).

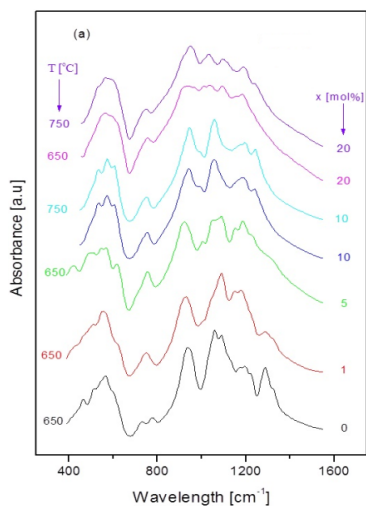


**Figure 4.** The FTIR spectra for the studied glass ceramics

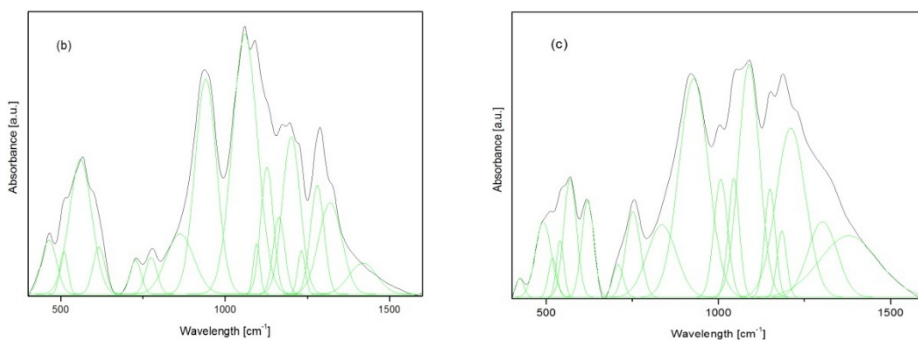


**Figure 5.** The deconvoluted FTIR spectra for a) the glass ceramic matrix and b) for the sample doped with  $x = 5$  mol% of iron(III) oxide

The assignments for the IR vibrations of the studied samples are listed in table 3.

Analyzing the FTIR spectra of the thermally treated samples can be observed the fact that are more solved than those of the thermally untreated samples [25]. Due to the fact that a solved spectrum correspond to an ordered structure according with literature [25] our obtained samples present a more ordered structure than the thermally untreated samples.

By increasing the concentration of iron(III) oxide the FTIR peaks became broad (see figure 4), due to some structural changes in the network (increase the number of non-bridging oxygen atoms). These changes correspond to a more disordered structure, similar with the case of the untreated samples [25]. The IR results are in agreement with the other obtained data.

**Table 3.** The assignments, of the IR vibration for the annealed samples from the glass ceramic system  $(\text{Fe}_2\text{O}_3)_x \cdot (\text{P}_2\text{O}_5)_{40} \cdot (\text{ZnO})_{(60-x)}$ 

Wavenumber [ $\text{cm}^{-1}$ ]	Assignment	Reference
424-497	$\delta$ (O=P-O)	[26]
503-518	Zn-O in $\text{ZnO}_4$ units	[27]
535-559	$\delta$ (O-P-O)	[28, 29]
560-569	$\nu$ (Fe-O) in $\text{FeO}_4$ units	[30, 31, 32]
604-625	$\nu$ (Zn-O) in $\text{ZnO}_4$ units	[27, 33, 34]
706-727	$\nu_s$ (P-O-P)	[35]
739-779		
812-862	$\nu_{as}$ (P-O-P)	[36]
927-948		
988-1006	$\nu$ (P-O <sup>-</sup> ) ( $\text{Q}^0$ )	[37]
1036-1059	$\nu$ ( $\text{PO}_3$ ) <sup>2-</sup> ( $\text{Q}^1$ )	[38, 39]
1089-1127	$\nu_{as}$ ( $\text{PO}_4$ ) <sup>3-</sup> ( $\text{Q}^0$ )	[38, 39]
1138-1163	$\nu$ ( $\text{PO}_2$ ) <sup>-</sup> ( $\text{Q}^2$ )	[38, 39]
1184-1201	$\nu_{as}$ ( $\text{PO}_2$ ) ( $\text{Q}^2$ )	[37]
1210-1247		
1277-1321	$\nu_{as}$ (P=O)	[39]
1355-1419	$\nu_s$ (P=O)	[28]

Legend:

- $\delta$ - bending vibrations
- $\nu$ - stretching vibrations
- $\nu_{as}$ - asymmetric stretching vibrations
- $\nu_s$ - symmetric stretching vibrations

Concluding, the thermal treatment lead to the changes in the glass ceramic network for example the formation of the  $\text{ZnO}_4$  units, which are not present in the glass ceramic network of the untreated samples [25].

## CONCLUSIONS

Some glass ceramic samples with stoichiometric composition  $(\text{Fe}_2\text{O}_3)_x \cdot (\text{P}_2\text{O}_5)_{40} \cdot (\text{ZnO})_{(60-x)}$  were obtained by melt-quenching technique followed by a heat treatment for two hours at 650 and 750 °C.

The DTA measurements show that with increasing in concentration of the iron(III) oxide ( $\text{Fe}_2\text{O}_3$ ) the transition and crystallization temperatures increase also. The glass matrix present the highest stability and by increasing of the doping level the stability of glass (TS, S) decreases probably by the increasing of the non-bridging oxygen number from the glass network.

The XRD data for the thermally treated samples show the presence of two or three crystalline phases in the studied samples.

The thermal treatment lead to the formation of  $ZnO_4$  and  $FeO_4$  units confirmed by the FTIR data. Also the FTIR spectra of the samples thermally treated are more solved, this mean a more ordered structure.

In conclusion all the obtained data confirm that the thermal treatment lead to the changes in the glass ceramic network, the structure becoming more ordered, that in the case of the untreated samples.

## EXPERIMENTAL SECTION

Samples, using the melt-quenching technique, corresponding to the glass ceramic system  $(Fe_2O_3)_x \cdot (P_2O_5)_{40} \cdot (ZnO)_{(60-x)}$  were obtained. The starting materials used ( $Fe_2O_3$ ,  $P_2O_5$ ,  $ZnO$ ) were of high purity Alfa Aesar (99.9 %). The stoichiometric amounts of these oxides were mixed and homogenized into an agate mortar. The mixtures were melted using a porcelain crucible at  $1100\text{ }^\circ\text{C}$  for 15 minutes using an electric furnace. Then the molten material was quickly cooled at room temperature by pouring onto a stainless-steel plate. After that the samples were thermally treated for two hours at different temperatures 650 and  $750\text{ }^\circ\text{C}$ .

The DTA data were obtained using a PerkinElmer TG/DTA 6300 thermal analyzer under argon gas atmosphere.

The XRD measurements were carried out using a XRD-6000 Shimadzu diffractometer, with a graphite monochromator  $Cu-K_\alpha$  radiation ( $\lambda = 1.54\text{ \AA}$ ) at room temperature.

The FTIR spectra were done using a FTIR apparatus (JASCO FTIR 6200 spectrometer) in the  $400\text{-}1800\text{ cm}^{-1}$ . The spectra were registered using KBr pellets.

## REFERENCES

- [1]. G. Kumar, S.K. Apte, S.N. Garaje, M.V. Kulkarni, S.M. Mahajan, B.B. Kale, *Applied Physics A-Materials Science & Processing*, **2010**, 98, 531.
- [2]. J.C. Knowles, *Journal of Materials Chemistry*, **2003**, 13, 2395.
- [3]. V. Rajendran, A.V. Gayathri Devi, M. Azooz, F H. El-Batal, *Journal of Non-Crystalline Solids*, **2007**, 353, 77.
- [4]. A. Pan, A. Ghosh, *Journal of Materials Research*, **2002**, 17, 1941.
- [5]. A.A. Bahgat, B.A.A. Makram, E.E. Shaisha, M.M. El-Desoky, *Journal of Alloys and Compounds*, **2010**, 506, 141.
- [6]. R.K. Singh, A. Srinivasan, *Journal of Magnetism and Magnetic Materials*, **2010**, 322, 2018.
- [7]. B.C. Sales, L.A. Boatner, *Materials Letters*, **1984**, 2(4B), 301.

- [8]. P.I. Paulose, G. Jose, N.V. Unnikrishnan, *Journal of Non-Crystalline Solids*, **2010**, 356, 93.
- [9]. B. Kang, G. Ceder, *Nature*, **2009**, 458, 190.
- [10]. B. Tischendorf, J.U. Otaigbe, J.W. Wiench, M. Pruski, B.C. Sales, *Journal of Non-Crystalline Solids*, **2001**, 282, 147.
- [11]. U. Caldino, E. Alvarez, A. Speghini, M. Bettinelli, *Journal of Luminescence*, **2013**, 135, 216.
- [12]. M.G. Mesko, D.E. Day, *Journal of Non-Crystalline Solids*, **1999**, 27, 327.
- [13]. A. Mogusmilankovic, V. Licina, S.T. Reis, D.E. Day, *Journal of Non-Crystalline Solids*, **2007**, 353, 2659.
- [14]. J.F. Duce, J.J. Videau, *Materials Letters*, **1992**, 13, 271.
- [15]. L. Koudelka, P. Mosner, *Materials Letters*, **2000**, 42, 194.
- [16]. M.K. Hwang, B.K. Ryu, *Journal of the Korean Physical Society*, **2016**, 69, 157.
- [17]. P. Pascuta, M. Bosca, G. Borodi, E. Culea, *Journal of Alloys and Compounds*, **2011**, 509, 4314.
- [18]. A. Dietzel, *Glastechnische Berichte-Glass Science and Technology*, **1968**, 22, 41.
- [19]. A. Hruby, *Physica B*, **1972**, 22, 1187.
- [20]. M. Saad, M. Poulin, *Materials Science Forum*, **1987**, 19-20, 11.
- [21]. N. Mehta, R.S. Tiwari, A. Kumar, *Materials Research Bulletin*, **2006**, 41, 1664.
- [22]. H.E. Kissinger, *Analytical Chemistry*, **1957**, 29, 1702.
- [23]. N.S. Saxena, *Journal of Non-Crystalline Solids*, **2004**, 345-346, 161.
- [24]. *Accelrys Software Inc. Materials Studio, Release 5.5. 2010.*
- [25]. P. Pascuta, G. Borodi, A. Popa, V. Dan, E. Culea, *Materials Chemistry and Physics*, **2010**, 123, 767.
- [26]. H. Doweidar, Y.M. Moustafa, K. El-Egili, I. Abbas, *Vibrational Spectroscopy*, **2003**, 339, 83.
- [27]. E. Mansour, G. El-Damrawi, *Physica B*, **2010**, 405, 2137.
- [28]. D.A. Magdas, O. Cozar, V. Chis, I. Ardelean, N. Vedeanu, *Vibrational Spectroscopy*, **2008**, 48, 251.
- [29]. P. Pascuta, G. Borodi, N. Jumate, I. Vida-Simiti, V. Dan, E. Culea, *Journal of Alloys and Compounds*, **2010**, 504, 479.
- [30]. M.G. Ferreira da Silva, B.F.O. Costa, *Journal of Non-Crystalline Solids*, **2001**, 293-295, 534.
- [31]. I. Ardelean, R. Lungu, P. Pascuta, *Journal of Materials Science - Materials in Electronics*, **2007**, 18, 837.
- [32]. I. Ardelean, P. Pascuta, *Materials Letters*, **2004**, 58, 3499.
- [33]. H.S. Liu, T.S. Chin, S.W. Yung, *Materials Chemistry and Physics*, **1997**, 50, 1.
- [34]. P. Pascuta, E. Culea, *Journal of Materials Science - Materials in Electronics*, **2011**, 22, 1060.
- [35]. P. Subbalakshmi, N. Veeraiah, *Journal of Non-Crystalline Solids*, **2002**, 298, 89.
- [36]. B.H. Jung, D.N. Kim, H.S. Kim, *Journal of Non-Crystalline Solids*, **2005**, 351, 3356.
- [37]. Y.M. Lai, X.F. Liang, S.Y. Yang, J.X. Wang, L.H. Cao, B. Dai, *Journal of Molecular Structure*, **2011**, 992, 84.
- [38]. L. Baia, M. Baia, W. Kiefer, J. Popp, S. Simon, *Chemical Physics*, **2006**, 327, 63.
- [39]. S. Marzouk, *Materials Chemistry and Physics*, **2009**, 114, 188.